



*sustainability*



Article

---

# Using the DTFM Method to Analyse the Degradation Process of Bilateral Trade Relations between China and Australia

---

Xiaoyang Han, Sijing Ye, Shuyi Ren and Changqing Song

Special Issue

Geographic Information Science for the Sustainable Development

Edited by


Dr. Shi Shen, Dr. Peichao Gao and Dr. Shaohua Wang



<https://doi.org/10.3390/su15097297>

## Article

# Using the DTFM Method to Analyse the Degradation Process of Bilateral Trade Relations between China and Australia

Xiaoyang Han <sup>1</sup>, Sijing Ye <sup>1,2</sup> , Shuyi Ren <sup>1</sup> and Changqing Song <sup>1,2,\*</sup>

<sup>1</sup> Faculty of Geographical Science, Beijing Normal University, Beijing 100875, China; 202011051032@mail.bnu.edu.cn (X.H.); yesj@bnu.edu.cn (S.Y.); 202021051058@mail.bnu.edu.cn (S.R.)

<sup>2</sup> State Key Laboratory of Earth Surface Processes and Resource Ecology, Beijing Normal University, Beijing 100875, China

\* Correspondence: songcq@bnu.edu.cn

**Abstract:** Quantitative assessment and visual analysis of the multidimensional features of international bilateral product trade are crucial for global trade research. However, current methods face poor salience and expression issues when analysing the characteristics of China—Australia bilateral trade from 1998 to 2019. To address this, we propose a new perspective that involves period division, feature extraction, construction of product space, and spatiotemporal analysis by selecting the display competitive advantage index using the digital trade feature map (DTFM) method. Our results reveal that the distribution of product importance in China—Australia bilateral trade is heavy-tailed, and that the number of essential products has decreased by 68% over time. The proportion of products in which China dominates increased from 71% to 77%. Furthermore, Australia consistently maintains dominance in the most crucial development in trade, and the supremacy of the head product is becoming stronger. Based on these findings, the stability of bilateral trade between Australia and China is declining, and the pattern of polarisation in the importance of traded products is worsening. This paper proposes a novel method for studying Sino—Australian trade support. The analytical approach presented can be extended to analyse the features of bilateral trade between other countries.

**Keywords:** geographic information science; spatial thinking; heavy-tailed distribution; k-means clustering; co-clustering algorithm; geovisualisation



**Citation:** Han, X.; Ye, S.; Ren, S.; Song, C. Using the DTFM Method to Analyse the Degradation Process of Bilateral Trade Relations between China and Australia. *Sustainability* **2023**, *15*, 7297. <https://doi.org/10.3390/su15097297>

Academic Editor: Jacob Arie Jordaan

Received: 20 March 2023

Revised: 18 April 2023

Accepted: 24 April 2023

Published: 27 April 2023



**Copyright:** © 2023 by the authors. Licensee MDPI, Basel, Switzerland. This article is an open access article distributed under the terms and conditions of the Creative Commons Attribution (CC BY) license (<https://creativecommons.org/licenses/by/4.0/>).

## 1. Introduction

In the era of economic globalisation, trade between countries is essential in promoting national economic growth and social development [1]. The development of trade research between countries plays an essential role in interpreting trade structure, evolutionary development, and driving factors. Among them, the research and application of methods for the quantitative assessment of the multidimensional characteristics of international bilateral product trade is a vital topic in international trade research. These methods are crucial for understanding the development process of bilateral trade and exploring sustainable industrial transformation paths.

The current academic approaches to the quantitative assessment of international bilateral product trade characteristics can be divided into three main categories: trade characteristic index methods, virtualisation methods of product trade flows, and spatiotemporal statistical methods represented by complex networks and gravity models. First, several trade characteristic indices extracted from classical trade theories are widely used to characterise international bilateral product trade. For example, Wu et al. expanded the assessment of global digital competitiveness based on the traditional international competitiveness diamond model. They concluded that the top 30 countries worldwide have more substantial integrated digital competitiveness [2]. Han et al. used the data of UN Comtrade to measure the trade integration index of China and West Asia, the

Grubel—Lloyd intra-industry trade index, and the Brehart marginal intra-industry trade index, and they revealed a comparative advantage index, concluding that China's trade with West Asia is becoming closer. Trade complementarity is more substantial and falls within the policy expectation that China will strengthen trade cooperation with these regions in the context of the Belt and Road Initiative [3]. Casanova used the export dependence index to measure the relative exposure of various Latin American countries to fluctuations in demand for Chinese products [4]. Zhang et al. analysed the changes in China's trade dependence with Belt and Road countries through the composite trade share index, the trade closeness index, and the HM index, and with the help of quantitative models such as the gravity model they concluded that geographical distance and economic size are the main influences on China's trade dependence with its trading partners [5]. Multidimensional indices such as the trade complementarity index and the trade closeness index are widely used to analyse the competitiveness of a country's industry, the country's position in the international trade industry value chain, and the degree of dependence on other trading partners [2,3,5–7]. However, most indices originating from economics and management only focus on the industrial linkages between one another within a pair of countries or a region. Fewer studies comprehensively portray the industrial relations among the world's significant economies [8]. Most of the trade products that they analyse are one product or one type, which is often limited by the smoothing of trade product information and fails to highlight critical products when comprehensively analysing multiple products over a long period.

Second, the trade flows of products have been virtualised in numerous studies to analyse the resource flows and their ecological impacts resulting from product trade. Thus, they rationalise regional development and resource management from environmental and economic perspectives [9,10]. For example, virtual water and land resources hidden in products and services move between regions in the trade process [11]. Yu et al. found that the China—Pakistan food trade both enhances Pakistan's economy and is equivalent to the net import of food produced on 520,000 hm<sup>2</sup> of arable land in China, thereby alleviating China's growing arable land crisis by examining market integration and calculating the flows of virtual land and virtual water resources [12]. Sun et al. analysed the virtual water input and output of the Qinghai—Tibet Plateau by constructing a complex network and a logarithmic mean Divisia index (LMDI) model, and they concluded that it exports a net 225 million m<sup>3</sup> of virtual water to the outside world to relieve water stress in other regions [13]. Carbon emissions from production and service processes are often studied as indicators of environmental and ecological conservation; for example, Hertwich and Peters et al. calculated the per capita carbon emissions of each country by quantifying the greenhouse gas emissions associated with the consumption of final goods and services in 73 countries and 14 regions [14]; thus, the database was used to quantify the transfer of emissions through international trade to explore the vital implications of international work on carbon emissions in each country and, therefore, to call for energy savings and emission reductions [15]. Through virtualising trade product flows, researchers can explain the resource flows behind product trade and, thus, provide feasible solutions to solve the ecological crisis and alleviate resource shortages. However, current product studies mainly focus on primary products related to resources and ecology. There needs to be a more systematic analysis of various types of trade products from a global perspective.

Third, since Barabasi and Albert [16] proposed a scale-free network model with a power-law distribution of nodes at the end of the last century, complex network models have been widely used to reveal the structure of trading partners and the evolution of trade patterns based on their similarity to real-world trade networks [17]. In recent years, most studies have used countries or regions as network nodes [17–19], with trade flows as edges, the number of trade objects in a country or region as nodal degrees, and the magnitude of trade volumes and trade indices as weights, to express the trade characteristics, drivers, and the process of change in the international trading system between countries and regions for such types of products as food [20], iron ore [17,21], and medical devices [22]. For

example, Xu et al. analysed the high-end manufacturing trade patterns of countries along the Belt and Road using exponential random graphs based on complex networks. They found that China, India, and Singapore are in important node positions in this network, while North and Central Asian countries are in relatively marginal areas, leading to the conclusion that the interchange of this network still needs to be improved, along with trade and financial/monetary freedom. Furthermore, government effectiveness has a significant positive contribution to high-end manufacturing trade [23]. Dong analysed the impact of climate change on global wheat trade flows by constructing a competitive wheat trade network and, ultimately, proposed a policy framework to promote a stable and healthy wheat trade environment [19]. After the COVID-19 outbreak, Coquide analysed the multiproduct World Trade Network (WTN) for 2018–2020 on a Google Analytics matrix constructed by Ermann based on the high nestedness of trade networks [24], to explore the dramatic impact of the COVID-19 outbreak on the international trade balance [25]. Product flows and trade structures among trading partners can be revealed with the help of complex network analysis. Nevertheless, only one product type can often be analysed, and the number of products becomes a limitation of these studies. With the deepening of research, economic geographers have found that product linkages and technological linkages have significant impacts on the structure of regional product production and development in a region [26], and Hidalgo [27] and others proposed the concept of “product space” to portray the technological linkage networks between products and tandem production products through product trade data. The spatial distribution of products in this bimodal network is heterogeneous, with essential and closely linked products constituting the “core area”, and less-connected products constituting the “periphery area”. On this basis, Hausmann et al. combined product space with economic complexity and comparative advantage theory, arguing that products are a reflection of the potential and strength of countries and regions, and concluding that countries that focus on the spatially dense part of products are more likely to reveal their comparative advantage than those that concentrate on unrelated products [28]. However, constructing trade networks that can analyse hundreds of products at a time is too complex. It is challenging to identify and visualise specific products among such trade networks; this, in turn, makes it difficult to clearly express the differences in trade characteristics between countries or different periods, while complex networks that rely on economic models can only discuss trade relationships from a single perspective, making it challenging to reflect the complexity and dynamics of existing trade networks [29–32]. In response to the shortcomings of the above methods for expressing the characteristics of the interaction of a large number of products in bilateral trade, Ye et al. proposed a method for describing and analysing the “spatial pattern” of a large number of types of products from a spatial perspective, using the digital trade feature map (DTFM) and a general application framework. On this basis, the DTFM method was applied to analyse the characteristics of bilateral trade between China and the United States [32,33], and the method showed the advantages of being highly expandable, well-expressed, and easy to operate.

Research on China—Australia trade focuses on “analysis of the overall trade relationship between China and Australia”, “analysis of specific products of China—Australia trade”, and “analysis of trade links between China-Australia trade and third parties”. In the analysis of the overall trade relationship between China and Australia, researchers have used the nature of trade—such as dependence [34], complementarity [35], and structure [36]—to obtain the characteristics of the close ties and interdependence between China and Australia. Nevertheless, Australia is too dependent on Chinese manufacturing goods. In the prospective analysis, researchers focus on the establishment of a China—Australia free trade area [37,38] and the deepening of the trade war [39] to explore where China and Australia will go on the trade road. In the product-specific analysis of China—Australia trade, researchers focus on essential commodities in China—Australia trade—such as agricultural products [30,40], livestock products [41,42], and iron ore [43]—and evaluate the fluctuation of trade intensity of these crucial commodities over time, along with the domi-

nance overdependence in bilateral trade. Among the trade links between China—Australia trade and third parties, existing studies have focused on the comparative analysis of China—Australia trade with other economies, e.g., with other Asian countries [44], with other Oceanian countries [45], and with the world as a whole [46]. In the existing studies of bilateral trade between Australia and China, researchers tend to analyse only one type of commodity. The overall analysis is mainly limited to exploring the changes in trade indicators while neglecting the visual representation of the overall trade pattern.

In this study, the display competitive advantage index and DTFM methods were integrated and applied to analyse the changing features of bilateral trade between Australia and China for 1256 products from 1998 to 2019. First, the CA index of each product was calculated to characterise its competitive advantage in the bilateral trade between Australia and China. The trade space was established by taking the product's CA index in China as the  $x$ -axis and the CA index in Australia as the  $y$ -axis. The annual characteristics of each product in China—Australia bilateral trade were expressed as “points”. The co-clustering algorithm was applied to divide the CA index of China—Australia trade products into four periods (i.e., 1998–2002, 2003–2006, 2007–2010, and 2011–2019) according to their various characteristics. Second, based on the time-sharing results, standard deviation ellipses were constructed based on the set of “points” in the trade space for each product at a particular time. The length of the line from the ellipse's centre to the origin and the angle between the bar and the positive direction of the  $x$ -axis indicate the importance and competitiveness indices of the product category in that period, respectively. The head/tail breaks method was applied to classify the rank—size distribution of importance indices into five levels, with a power-law distribution spatial pattern. Subsequently, the overall trade characteristics of China—Australia bilateral trade and its strength and dominance over time were analysed. Finally, we discussed the patterns of changes in the importance and competitiveness of products and the analysis of changes in the importance and substitutability of head products in trade. This study looks at China and Australia and identifies trends in bilateral trade degradation and key trade characteristics over the past 20 years, which are essential for understanding the product trade relationship between China and Australia and revealing the bilateral trade patterns between the two countries from a holistic perspective. At the same time, the analytical approach of this paper provides a more straightforward analysis and representation of the overall pattern of bilateral trade and the evolution of a variety of products, which can provide a broader perspective for understanding trade characteristics and can provide methodological support for optimising trade structures and, thus, exploring sustainable development paths for bilateral trade, and can be extended to analyse the characteristics of bilateral trade between other countries.

## 2. Materials and Methods

### 2.1. Dataset Source

The United Nations Comtrade Dataset “<http://comtrade.un.org> (accessed on 1 February 2021)” is the world's largest and most widely used international trade database, with high authority and integrity. It provides essential data and application support for enriching trade theory, developing international trade characteristic quantity measures, and describing changes in global trade patterns. It is widely used in geographic studies because of its global perspective [47]. The earliest record in the database dates back to 1962, and more than 3 billion trade data from all countries worldwide have been stored thus far. More than 200 countries and regions in the repository remit annual international trade statistics based on goods, service categories, and trading partner countries. These data are then converted to UNSD standard formats such as the Harmonized System of Product Description and Coding (HS), Standard International Trade Commodity Classification (SITC), and Classification by Broad Economic Categories (BEC) during the loading, analysis, and evaluation of the data. This paper extracts the annual product trade dataset of China and Australia from the UN Comtrade Dataset. The dataset covers the annual import and export trade

of traded products between China and Australia from 1998 to 2019 (in USD). All traded products were classified and coded according to the HS 4-digit coding rules, totalling 1256.

## 2.2. Displayed Competitive Comparative Advantage Index (CA)

The index of competitive advantage (CA) was proposed by Vollrath et al. [48], and it expresses the real competitive advantage of a country for a product by subtracting the comparative advantage of imports from the comparative advantage of a country's exports. As shown in Equation (1),  $RCA_{ij}$  denotes the revealed comparative advantage of country  $i$  in product  $j$ , where  $X_{ji}$  denotes the export value of country  $i$ 's export good  $j$ ,  $X_{ti}$  denotes the export value of country  $i$ , and  $X_{jw}$  denotes the export value of world export good  $j$ .  $X_{tw}$  denotes the total export value of world export goods.  $M_{ji}$  denotes country  $i$ 's imports of product  $j$ ,  $M_{ti}$  denotes country  $i$ 's total imports in a period,  $M_{jw}$  denotes imports on the world market for product  $j$  in the same period, and  $M_{tw}$  denotes the value of total imports on the world market in the same period. Supposing that  $CA > 0$ , the country's product exports in the period have a specific competitive advantage, which increases with the increase in CA. If  $CA = 0$ , it means that the country's product exports in the period do not have a competitive advantage or have no competitive disadvantage. If  $CA < 0$ , the country's product exports in the period have a particular competitive disadvantage, which increases with the decrease in CA. Finally, the co-clustering algorithm was used to classify the CA index of China—Australia trade products into four time periods by the China CA index value (i.e., 1998–2002; 2003–2006; 2007–2010; 2011–2019) (see the detailed classification results in Supplementary Materials S1).

$$CA_{ij} = RCA_{ij} - \frac{\frac{M_{ji}}{M_{ti}}}{\frac{M_{jw}}{M_{tw}}}, RCA_{ij} = \frac{\frac{X_{ji}}{X_{ti}}}{\frac{X_{jw}}{X_{tw}}} \quad (1)$$

Clustering is one of the most common methods in data mining. Compared with the traditional one-way clustering algorithm, which only considers data objects or attributes as features for similarity calculation, the -co-clustering algorithm takes data objects and attributes into account when clustering, making the results more meaningful [49]. Considering that the -co-clustering algorithm can quickly and efficiently identify and classify extensive data, we sorted the products in China from low to high according to the HS4CODE code. In the matrix composed of CA index values from 1998 to 2019, the rows of the matrix were used as data objects (that is, HS4CODE code, product type). The matrix's column attribute (CA index value of each year) was used for bidirectional clustering calculation. After comparing and analysing a variety of clustering schemes, we believed that dividing the time period into four categories—1998–2002, 2003–2006, 2007–2010, and 2011–2019—and dividing the products into 15 categories would best express the characteristics of CA differentiation between different products and different years (see the details in Supplementary Materials S2).

Figure 1 shows the results of some products divided in the time period after the -co-clustering algorithm, where the squares of different colours are used to show the value of the CA index of a product in a specific year, and the CA values of different products in different years in the same period are similar. The results show that the products in several groups—1 to 9, 10 to 19, and 40 to 49—all show a low CA index in all four periods. Most products in the 50 to 59 and 60 to 69 groups show relatively high CA index scores in all four periods. The time segmentation results adequately express the gradual increase in the CA index of some products in groups 20 to 29 and 80 to 89.

## 2.3. Trade Data Spatialisation Method

Ye et al. proposed a trade space based on the expression of geographic space, which reflects the changing characteristics and relevance of trade goods through the relationship of points and lines in the Cartesian coordinate system [32,33]. This paper uses the following main steps to develop this approach in the face of a multistage trade analysis between the

two countries over a long period. First, products of different types and years are spatially transformed into a point set in a Cartesian coordinate system, using the displayed CA index as the coordinate axis. The horizontal coordinate of each product point is used to represent the CA value of the product in China in a given year. In contrast, the vertical coordinate represents the product's CA value in Australia in the same year. The location of the product points reflects the difference between the CA values of China and Australia for the product in a given year. Moreover, the dispersion of the point distribution reflects the degree of variation in the CA indices of China and Australia during the time period. Taking Figure 2 as an example, the light grey dots are the positions of the CA indices in the coordinate system for each product in each year shown, such as for product P (natural honey, HS4CODE = 0409);  $X_{Pi}$  and  $Y_{Pi}$  denote the Chinese CA index value and the Australian CA index value for this product in year  $i$ , respectively, while  $\bar{X}_{Pi}$  and  $\bar{Y}_{Pi}$  denote the average values of the Chinese and Australian CA indices over  $n$  years, which is the number of years in the corresponding time period. Standard deviation ellipses are used to quantitatively explain the holistic characteristics of the spatial distribution of economic factors in terms of centrality, spreading, directionality, and spatial patterns from a global and spatial perspective [50]. The ellipses of different colours in Figure 2 represent the directional distribution of each product at different time periods, where period 1 is orange, period 2 is green, period 3 is purple, and period 4 is blue. Taking product P in time period  $i$  as an example, its standard deviation ellipse centre coordinates are  $(\bar{X}_{Pi}, \bar{Y}_{Pi})$ . The length  $L(P, i)$  of the line connecting the ellipse's centre to the origin is defined as the average trade importance of product P in that time period, calculated by Equation (2). The angle  $A(P, i)$  between the centre of the ellipse and the line connecting the origin through the positive direction of the  $x$ -axis is defined as the average competitive advantage of product P during the time period and is calculated by Equation (3). If  $A(P, i)$  is within  $0\text{--}35^\circ$  or  $270\text{--}360^\circ$ , then it is class A, indicating that China has an advantage in the commodity trade in that period. Class B is in the range  $35\text{--}55^\circ$ , indicating that both countries have an equal advantage in the commodity trade in that period. Class C is in the range  $55\text{--}180^\circ$ , indicating that Australia has an advantage in the commodity trade in that period. Class D is in the range  $180\text{--}270^\circ$ , indicating that neither country has an advantage in the commodity trade in that period.

Through the above operation, the characteristics of each product's changes in CA values and their correlations and differences between one another in different time periods can be visually represented as spatial migration or aggregation. The differences in the CA index of each product and changes in the degree of dominance can be clearly expressed.

$$L(P, i) = \sqrt{\bar{X}_{Pi}^2 + \bar{Y}_{Pi}^2} \quad (2)$$

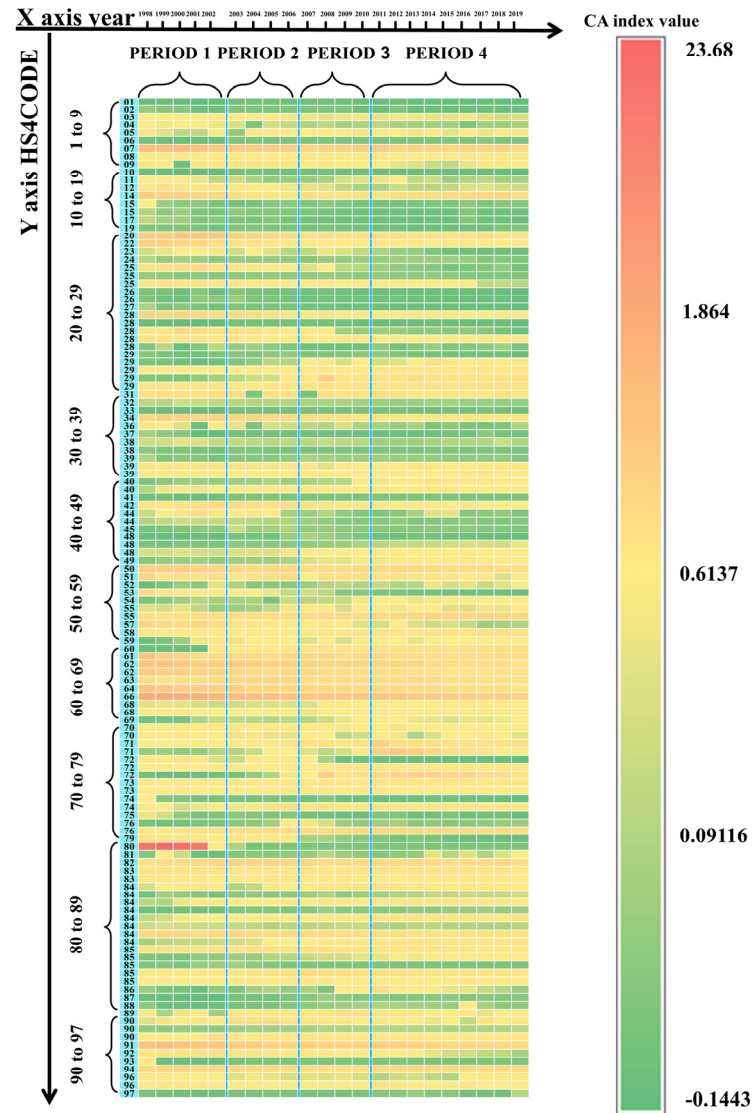
$$A(P, i) = \text{ATAN2}\left(\bar{X}_{Pi}, \bar{Y}_{Pi}\right) \quad (3)$$

Figure 3a shows the rank—size distribution of  $L(P, i)$  [51]. It shows a transparent heavy-tailed distribution [52], in which products with larger values have lower frequencies and constitute the “head”. In comparison, products with smaller values have higher frequencies and constitute the “tail”. Figure 3b shows the probability density function of  $L(P, i)$  in a logarithmic plot, where it is linear, and the distribution can be expressed as a power law.

#### 2.4. Trade Data Spatialisation Method

A heavy-tailed distribution is widely found in nature and human society. Unlike the standard normal distribution, it has a long tail that is always close to the  $x$ -axis, reflecting that a small number of essential individuals possess most of the overall “wealth”. For example, 20% of the society possesses 80% of the wealth, while the remaining 80% may only possess 20% of the wealth, or the internet head APP comprises the majority of internet users. Traditional methods for analysing heavy-tailed distributions are based on Gaussian analysis [53–55]. In these methods, researchers analyse the events that mainly focus on the high frequency of occurrence, while considering separating the events that occur less

frequently from them [56], which then forms the basis for the classification based on the natural breakpoint method [57]. However, low-frequency events often contain more critical information for heavy-tailed distributions and have higher importance than high-frequency events [58].



**Figure 1.** Heatmap of co-clustering algorithm results: All kinds of products are arranged according to HS4CODE, totalling 1256 items. One of every ten moderately spaced strips is selected and displayed with the first two bits of its code. The abscissa is sorted by year from 1998 to 2018, so each grid represents the CA index value of a specific type of product in China in a specific year. Periods 1, 2, 3, and 4 are 1998–2002, 2003–2006, 2007–2010, and 2011–2019, respectively.

Jiang et al. proposed a “head/tail breaks” method for filtering out the more critical “heads” from heavy-tailed distributions based on dividing the samples that fit the heavy-tailed distribution into two parts, using the sample mean as the threshold. The process continues iteratively for the head (i.e., the part above the mean) until the head is no longer in the heavy-tailed distribution. This method allows for a more natural and better-structured grouping or hierarchy of the heavy-tailed distribution data than natural breaks [59]. Taking Figure 4 as an example, the rank size of  $L(P, i)$  is divided into five classes (1, 2, 3, 4, and 5) by head-to-tail splitting;  $m_1, m_2, m_3,$  and  $m_4$  are the remaining sample means based on each head-to-tail split, and the higher class represents the more essential products in the foreign trade of China and Australia. The higher the  $L(P, i)$  rank, the less stable



the heavy-tailed distribution is after the power-law test. At rank E, the characteristics of the heavy-tailed distribution are less pronounced, and it becomes a significant linear distribution ( $R^2 = 0.82$ ). Considering the characteristics of the heavy-tailed distribution and the number of products in each rank, the segmentation is stopped. It can be concluded that there were five importance levels for each product in China—Australia trade.

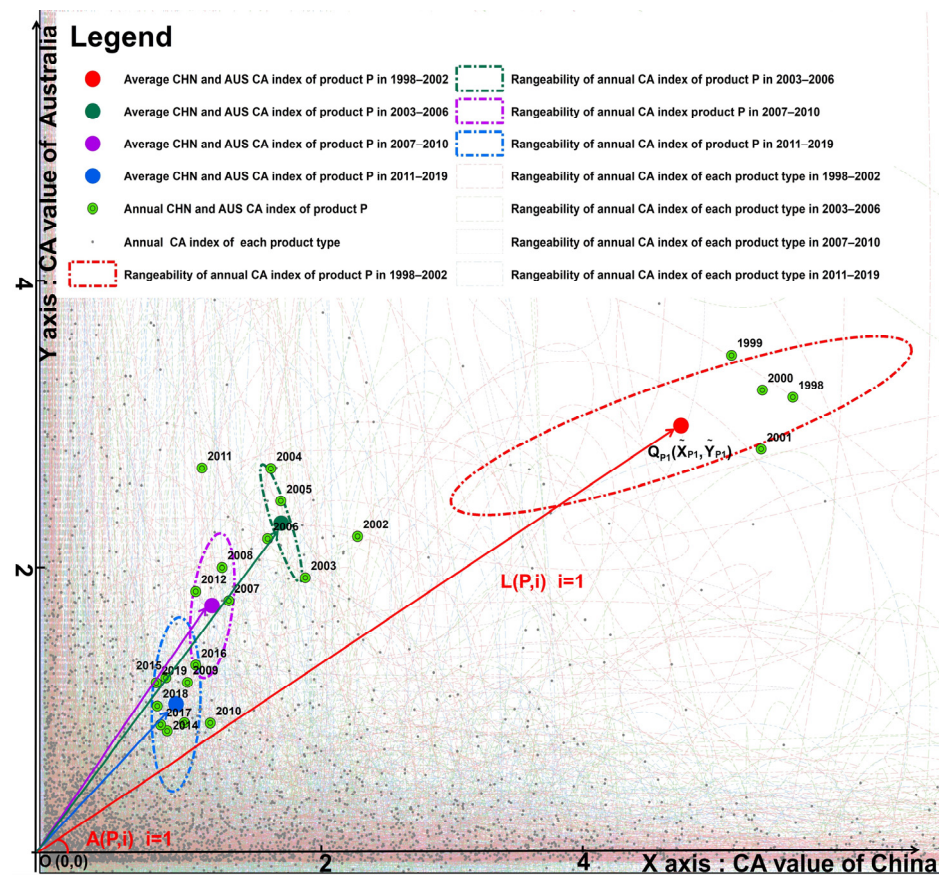


**Figure 2.** Variation in China and Australia trade in “trade space”: Product P represents “Natural honey”, and its HS 4-digit code is 0409. By creating a line that connects the original point O (0, 0) and central point  $Q_i(\bar{X}_{P_i}, \bar{Y}_{P_i})$ , the length of QO indicates the average trade importance of product P in time period 1. Angle A (P, i) between QO and the X-axis indicates the differences in the CA index between China and Australia.

### 2.5. Product Grid Generation Based on Hilbert Curves

A Hilbert curve is a continuous but non-derivative curve whose self-similarity property allows it to traverse all points in the unit square. Based on this property, the Hilbert curve can traverse every cell of any  $2^n \times 2^n$  square system and ensure that two cells adjacent to one another in the traversal order are also adjacent in real space. Due to the spatial correlation characteristics of geographic elements, Hilbert curves are widely used in the processing and management of geographic data. Ye et al. proposed a product grid generation method based on the inverse dimensional increase application of Hilbert curves [32], with the following main steps: The scanning matrix generation (SMG) method [60] is applied to construct the Hilbert curve and generate the  $n$ th-order ( $2^1 \times 2^1$ ) scan matrix  $H_2$  accurately and quickly, via an iterative algorithm based on the 1st-order ( $2^n \times 2^n$ ) matrix  $H_{2^n}$  according to the SMG, using Equation (4) as the formula. Therefore, for 1256 classes of goods encoded with HS4CODE, the four-bit encoding of the products can be mapped to two-dimensional space and spatially visualised in the network by applying SMG in reverse (see the detailed classification results in Supplementary Materials S3). Compared with the traditional Hilbert curve dimensionality reduction application, this reverse dimensionality increase method has

the advantages of wide application, high generality, and keeping the adjacency relationship before and after the transformation of adjacent elements. This paper uses the same method to construct a matrix for the visualisation and analysis of China—Australia trade.

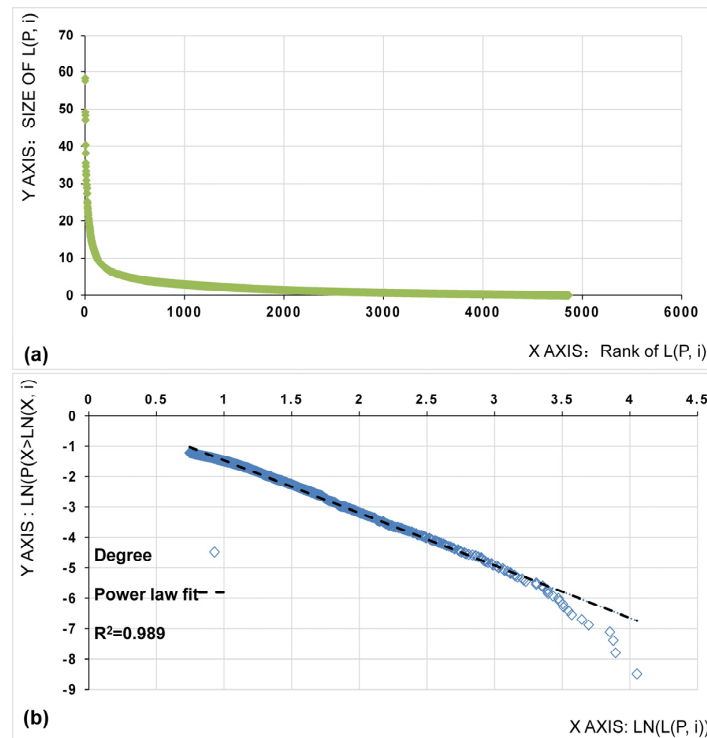


**Figure 3.** Heavy-tailed distributions of  $L(P, i)$ : (a) Rank—size distribution of  $L(P, i)$ . (b) Probability density distribution (Log) of  $L(P, i)$ .

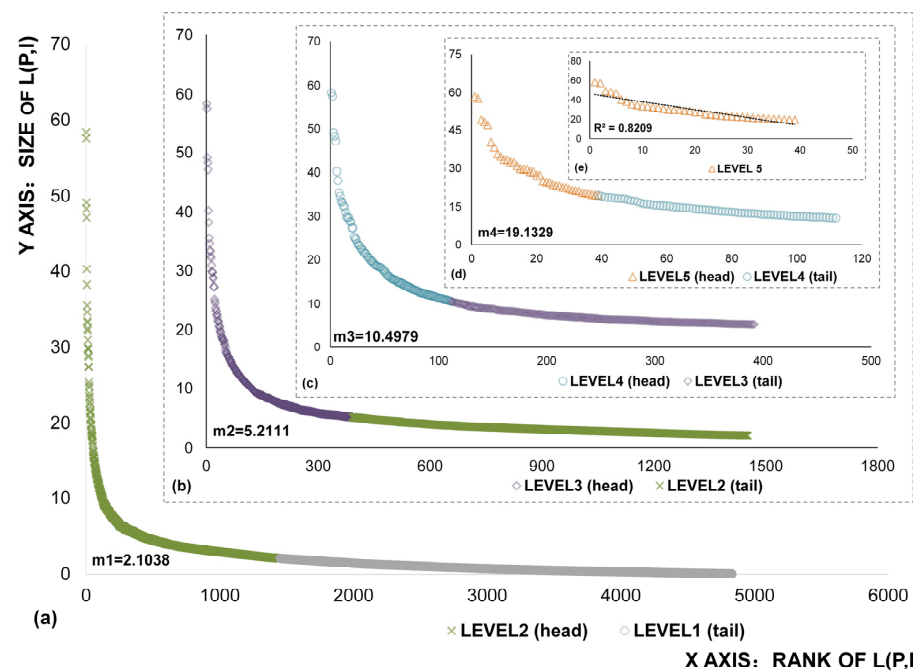


**Figure 4.** Classification process of the rank—size distribution of  $L(P, i)$  based on the head/tail breaks: (a) Level A and B products; (b) level B and C products; (c) level C and D products; (d) level D and E products; (e) level E products;  $m_1$ – $m_4$  represent the average value of each heavy-tailed distribution.

$$\begin{aligned}
 H_{2^{k+1}} = & \begin{cases} \begin{bmatrix} H_{2^k} & 4^k E_{2^k} + H_{2^k}^T \\ (4^k + 1)E_{2^k} - \overline{H_{2^k}} & (3 \times 4^k + 1)E_{2^k} - (\widetilde{H_{2^k}})^T \end{bmatrix} & \text{if } k \text{ is an even number} \\ \begin{bmatrix} H_{2^k} & (4^{k+1} + 1)E_{2^k} - \widetilde{H_{2^k}} \\ 4^k E_{2^k} + H_{2^k}^T & (3 \times 4^k + 1)E_{2^k} - (H_{2^k}^T) \end{bmatrix} & \text{if } k \text{ is an odd number} \end{cases} \\
 \text{thereunto, } H_2 = & \begin{bmatrix} 2 & 3 \\ 1 & 4 \end{bmatrix}, \text{ set } H_m = \begin{bmatrix} a_{1,1} & a_{1,2} & \dots & a_{1,m} \\ a_{2,1} & a_{2,1} & & a_{2,m} \\ \vdots & & \ddots & \vdots \\ a_{m,1} & a_{m,1} & \dots & a_{m,m} \end{bmatrix}, \\
 \widetilde{H}_m = & \begin{bmatrix} a_{1,m} & a_{1,m-1} & \dots & a_{1,1} \\ a_{2,m} & a_{2,m-1} & & a_{2,1} \\ \vdots & & \ddots & \vdots \\ a_{m,m} & a_{m,m-1} & \dots & a_{m,1} \end{bmatrix}, \overline{H}_m = \begin{bmatrix} a_{m,1} & a_{m,2} & \dots & a_{m,m} \\ a_{m-1,1} & a_{m-1,2} & & a_{m-1,m} \\ \vdots & & \ddots & \vdots \\ a_{1,1} & a_{1,2} & \dots & a_{1,m} \end{bmatrix}
 \end{aligned} \tag{4}$$

As shown in Supplementary Materials S3, commodities on the code are assigned to adjacent grids, and adjacent commodities in the trade code imply a high degree of similarity. For example, iron ore (HS4CODE = 2601) and manganese ore (HSCODE = 2602) both belong to ore and slag as well as ore ash (HS2CODE = 26), and both are close in the constructed Hilbert curve. This method makes it possible to analyse the characteristics of specific types of products and their neighbours to achieve an overall trade characterisation. This is not easy to achieve when applying other methods, such as those based on trade indicators or complex network analysis methods. In addition, based on the nature of the Hilbert curve inverse dimensioning that can fill any one-dimensional array, the method can be used to analyse the characteristics of any class of goods in any trade code, without considering changes in the type of goods and trade characteristics, making this method highly generalisable.

## 2.6. K-Means Clustering Algorithm

As the most popular clustering algorithm, the k-means clustering algorithm was first used by MacQueen in 1967 [61]. As a division-based, unsupervised learning clustering algorithm, k-means uses Euclidean distance to measure the similarity between individual objects. The smaller the distance between objects, the greater the similarity. The core idea is that  $k$  initial clustering centres  $C_i$  ( $1 \leq i \leq k$ ) are selected from the dataset. The Euclidean distance between the remaining objects in the dataset and the clustering centre  $C_i$  is calculated. Each object is assigned to the cluster corresponding to its closest clustering centre  $C_i$ . Finally, the mean value of data objects in each cluster is calculated as the new clustering centre. Iterations are continuously performed to update the clustering centre positions and the sum of squares due to error (SSE) of each cluster until the clustering centre. The sum of squared residuals no longer changes, or the maximum number of iterations is reached and stopped [62,63]. The Euclidean distance of each object in space from the cluster centre is calculated by Equation (5), and the sum of squares due to error (SSE) for the whole dataset is calculated using Equation (6):

$$d(x, C_i) = \sqrt{\sum_{j=1}^m (x_j - C_{ij})^2} \tag{5}$$

$$SSE = \sum_{i=1}^k \sum_{x \in C_i} |d(x, C_i)|^2 \tag{6}$$

where  $x$  is the object,  $C_i$  is the  $i$ th clustering centre,  $m$  is the dimension of the data object, and  $x_j$  and  $C_{ij}$  are the  $j$ th attribute values of  $x$  and  $C_i$ , respectively. The size of the SSE measures the clustering result, and  $k$  is the initial selection of clustering centres, which is the number of clusters.

The CA index of China—Australia trade products was divided into four time periods in this study to explore the patterns of trade characteristic quantities over time. K-means was used to cluster each characteristic trade quantity considering the time variation. The products were input as clustered objects. Their values and changes in  $L(P, i)$  and  $A(P, i)$  in different periods were used as the basis for classification, and the output was the pattern of changes in  $L(P, i)$  and  $A(P, i)$  of each product.

### 3. Results

#### 3.1. Temporal and Spatial Analysis of the “Average Importance Index”

In Figure 5a–d, CA-index-based trade feature maps are used to express each HS4CODE product's  $L(P, i)$  level in period 4 (2011–2019, Figure 5a), period 1 (1998–2002, Figure 5b), period 2 (2003–2006, Figure 5c), and period 3 (2007–2010, Figure 5d). Nearly 70.1% of level 1 product types (grey) constitute the tail, which supports the overall stability of China—Australia trade, while approximately 30% of level 2–5 products constitute the head, and more essential products (level 3–5) account for only 8% of all products. As shown in Figure 5a, most of the essential products in China—Australia trade ( $L(P, i)$  level = 4 or 5) are clustered in meat products (HS2CODE = 2) and ores (HS2CODE = 26), such as frozen sheep meat (HS4CODE = 0202), iron ores and concentrates (HS4CODE = 2601), aluminium ores and concentrates (HS4CODE = 2606), coal (HS4CODE = 2701), or aluminium oxide and other artificial corundum (HS4CODE = 2818). The more critical products in trade ( $L(P, i)$  level = 3) are more discrete in spatial distribution and are found in areas such as wood products (HS2CODE = 45), silk (HS2CODE = 50), and toys (HS2CODE = 95). In conclusion, the essential products in China—Australia trade mainly concentrate on labour-intensive products (e.g., grain, livestock, textiles) and capital-intensive products (e.g., ore, metallurgy). The reason for this distribution is that both China and Australia are rich in resources. For example, Australia has a vast natural endowment in the world's mineral and animal products. In contrast, China, as the “factory of the world”, has a tremendous competitive advantage in labour-intensive industries due to its abundant labour force. The pattern of essential products is relatively stable over time, but products with level  $L(P, i)$  level = 3 significantly weaken spatial agglomeration.

Figure 5e shows the changes in the number of “higher importance” products (i.e., level of  $L(P, i)$  equals 2–5) traded between China and Australia over the four time periods. The results show that the number of product categories with an importance level higher than three between China and Australia decreased significantly between 2003 and 2010. Among them, the number of products with importance level 3 decreased significantly from 100 in the first stage to 28 in the fourth stage—a decrease of 72%; the number of product categories with importance levels 4 and 5 also decreased from 33 and 10 to 12 and 6, respectively. This indicates that the close interdependence or competition between China and Australia in bilateral product trade has experienced a long-term decline over the past 20 years. More interestingly, the number of less-essential products (level 2) has increased over time, rising by approximately 10% over time, but not nearly as much as the decline in the higher-importance products (levels 3–5). This reflects the nature of the decline in bilateral trade between Australia and China as a “squeeze decline”, whereby many of the higher-ranked products have been declining in importance over time, leading to a sustained decline. The long-term decline is a counter-globalisation development process. At the same time, the role of bilateral trade relations between China and Australia in mitigating conflicts between the two countries has been declining.

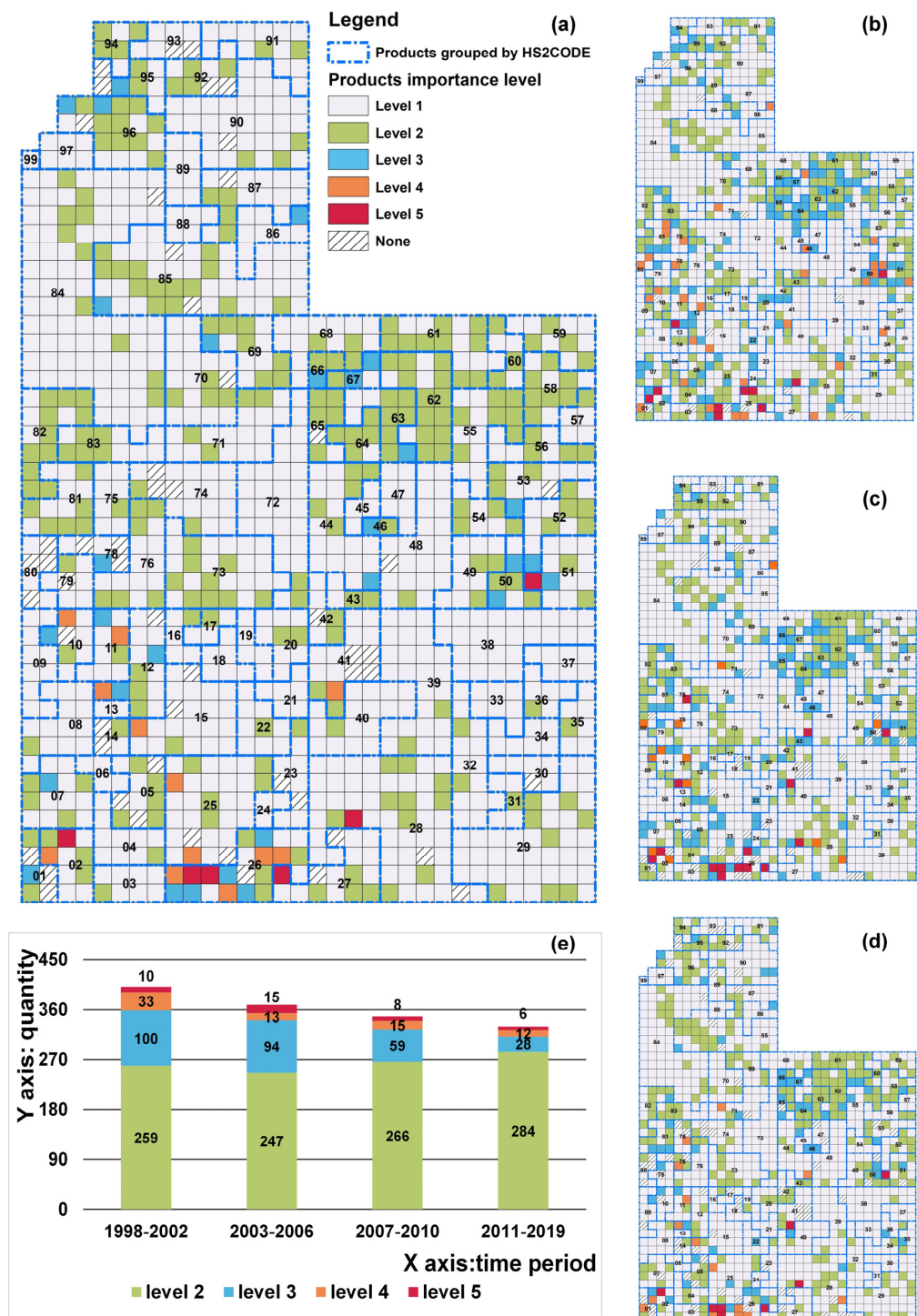


**Figure 5.** Spatial pattern of product L ( $P, i$ ) level in China–Australia bilateral trade: (a) Spatial pattern of product L ( $P, i$ ) level in China–Australia bilateral trade in time period 4 (2011–2019); (b) in time period 1 (1998–2002); (c) in time period 2 (2003–2006); (d) in time period 3 (2007–2010); (e) the histogram of the products in which L ( $P, i$ ) level  $\geq 2$  in each time period. Each lattice in the CA-index-based trade feature map corresponds to a specific HS4CODE product. The higher the level, the more important the product is in the trade between China and Australia. None means that the data for that product are missing at that time, possibly because some products were not assigned to HS4CODE at that time.

### 3.2. Temporal and Spatial Analysis of “Average Competitive Advantage”

The number of dominant products of both countries reveals the changes in the competitive nature of trade between China and Australia in the four periods. For the more essential products with  $L(P, i)$  level  $\geq 2$ , in Figure 6a–d, CA-index-based trade feature maps are used to express each HS4CODE product’s  $A(P, i)$  class in period 4 (2011–2019, Figure 6a), period 1 (1998–2002, Figure 6b), period 2 (2003–2006, Figure 6c), and period 3 (2007–2010, Figure 6d). Grids with different colours are used to map each product’s  $A(P, i)$  class at each time. The grids with orange colour represent the products for which China dominates in China–Australia trade at that time (class A), the green colour represents the products for which both countries are evenly matched at that time (class B), and the blue colour represents the products for which Australia dominates at that time (class C). The grey colour represents the products for which the  $L(P, i)$  class is deficient at that time, indicating that it does not contain much information. Figure 6e shows the change in the number of  $A(P, i)$  classes for the products with “higher importance” between China and Australia (i.e., level of  $L(P, i)$ ; Equations (2)–(5)) in the four periods. The number of products in class A is superior in each time period, and its overall proportion gradually expands. In contrast, the number of products in class C has a more apparent decreasing trend over time, which means that China has been occupying a dominant position in the trade competition between China and Australia, and its dominance has been increasing over time. Reflecting this in concrete terms, the number of products in which Australia was dominant fell by 29.5% in the final time period compared to the initial time period. In comparison, the number in which China was dominant fell by 12.8%. In the comparison between the two countries, the number of products in which China was dominant as a percentage of the total number of dominant products increased from 71.6% in the first time period to 77.3% in the final time period—further evidence of China’s growing dominance in bilateral trade.

In terms of spatial distribution, as shown in Figure 6a, the products of  $A(P, i)$  class C have an aggregated distribution, mainly concentrated in the areas of live animals (HS2CODE = 1), meat products (HS2CODE = 2), and ore slag (HS2CODE = 26), while there is a more discrete distribution in the areas of cereals (HS2CODE = 10) and hides and skins (HS2CODE = 41);  $A(P, i)$  class A products are clustered mainly in textile raw materials and textile products (HS2CODE = 50–63), handicraft products (HS2CODE = 64–67), ceramics (HS2CODE = 69), metal products (HS2CODE = 82–83) (HS2CODE = 85), toys (HS2CODE = 95), and electrical and electronic equipment and parts thereof. The pattern of the two countries’ products is relatively stable in all periods, indicating that the dominant products of bilateral product trade between China and Australia have not changed much in the past 20 years.

### 3.3. Comprehensive Temporal and Spatial Analysis of the “Average Importance Index and Competitive Advantage”

As shown in Figure 7a–d, the products’ importance levels and comparative advantages are represented synthetically on the grid by constructing a colour mapping space. The grey grid indicates that the  $L(P, i)$  level = 1 for the product in this time period, meaning that the product’s importance level is low and that it contains less information and has less impact on the overall pattern, so it is not analysed in detail. For the more essential products ( $L(P, i)$  level  $\geq 2$ ), different colours are used to indicate their  $A(P, i)$  class. Products with  $A(P, i)$  class A are indicated by the red colour scheme, which shows spatial clustering to a more considerable extent, and these products are mainly light industrial products, such as HS2CODE = 50–63 (textile raw materials and textile products), 81–83 (base metals and their products), 94–96 (miscellaneous articles), and other regions. These are mainly concentrated at the end of the value chain, with low market-access barriers and mainly labour-intensive industries, meaning that China is in the downstream of the world trade market and can only rely on its low labour costs to maintain a large number of exports of light industrial products. The products with  $A(P, i)$  class C are indicated by blue colour,

which are mainly animal products and ores, such as HS2CODE = 1 (live animals), 2 (meat and chop suey), and 26 (ore, slag, and ash), and these are more consistent with Australia's position as a significant energy and food exporter in global trade. In addition, there are only six products with the highest importance level ( $L(P, i)$  level = 5) in all periods—namely, HS4CODE = 0202 (meat of bovine animals, fresh or chilled), 0204 (lamb, fresh or chilled), 2601 (iron ores and concentrates, non-agglomerated; the average grain size no less than 0.8 mm, but no more than 6.3 mm), 2701 (anthracite, whether pulverised or not, but not agglomerated), 2818 (aluminium oxide, other than artificial corundum), and 5101 (greasy shorn wool, not carded or combed, in-quota)—and their  $A(P, i)$  classes are all C, which indicates that Australia has a tremendous advantage in the essential products in China–Australia trade. Supplementary Materials S4 shows the actual HS4CODE counterparts for products with higher  $L(P, i)$  levels in the first time period.

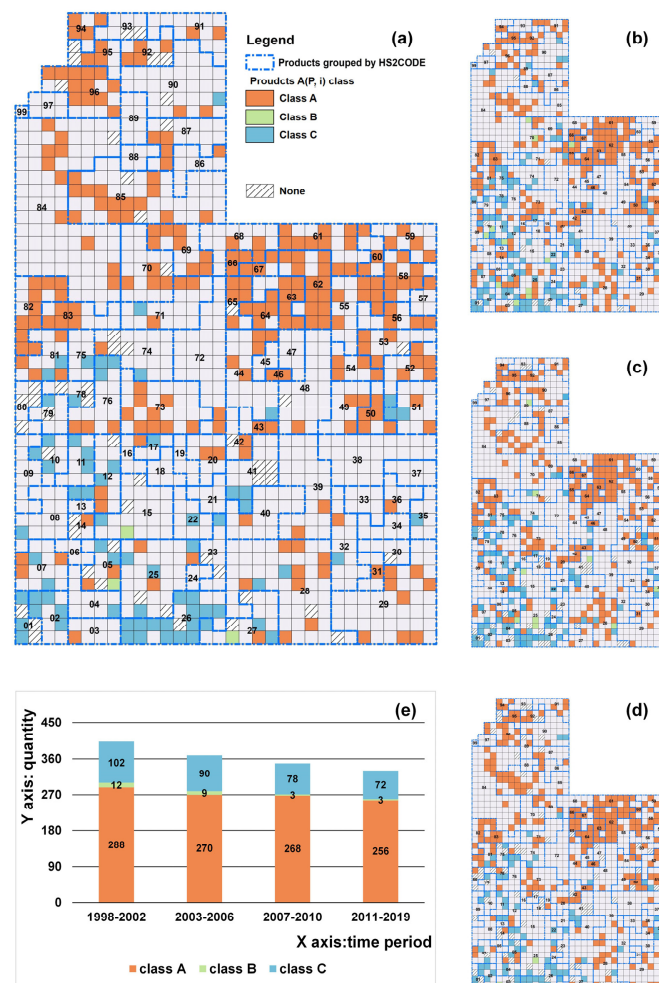


**Figure 6.** Spatial pattern of product  $A(P, i)$  classes in China–Australia bilateral trade: (a) Spatial pattern of product  $A(P, i)$  classes in China–Australia bilateral trade in time period 4 (2011–2019); (b) in time period 1 (1998–2002); (c) in time period 2 (2003–2006); (d) in time period 3 (2007–2010); (e) the histogram of the products'  $A(P, i)$  class in which  $L(P, i)$  level  $\geq 2$  in each time period. Each lattice in the CA-index-based trade feature map corresponds to a specific HS4CODE product. The orange grid means that China is dominant in the trade between China and Australia, the green grid means that there is a balance of power between the two countries, the blue grid means that Australia is dominant, and the grey grid means that the  $L(P, i)$  level of the corresponding product is too low to analyse. None means that the data for that product are missing at that time, possibly because some products were not assigned to HS4CODE at that time.

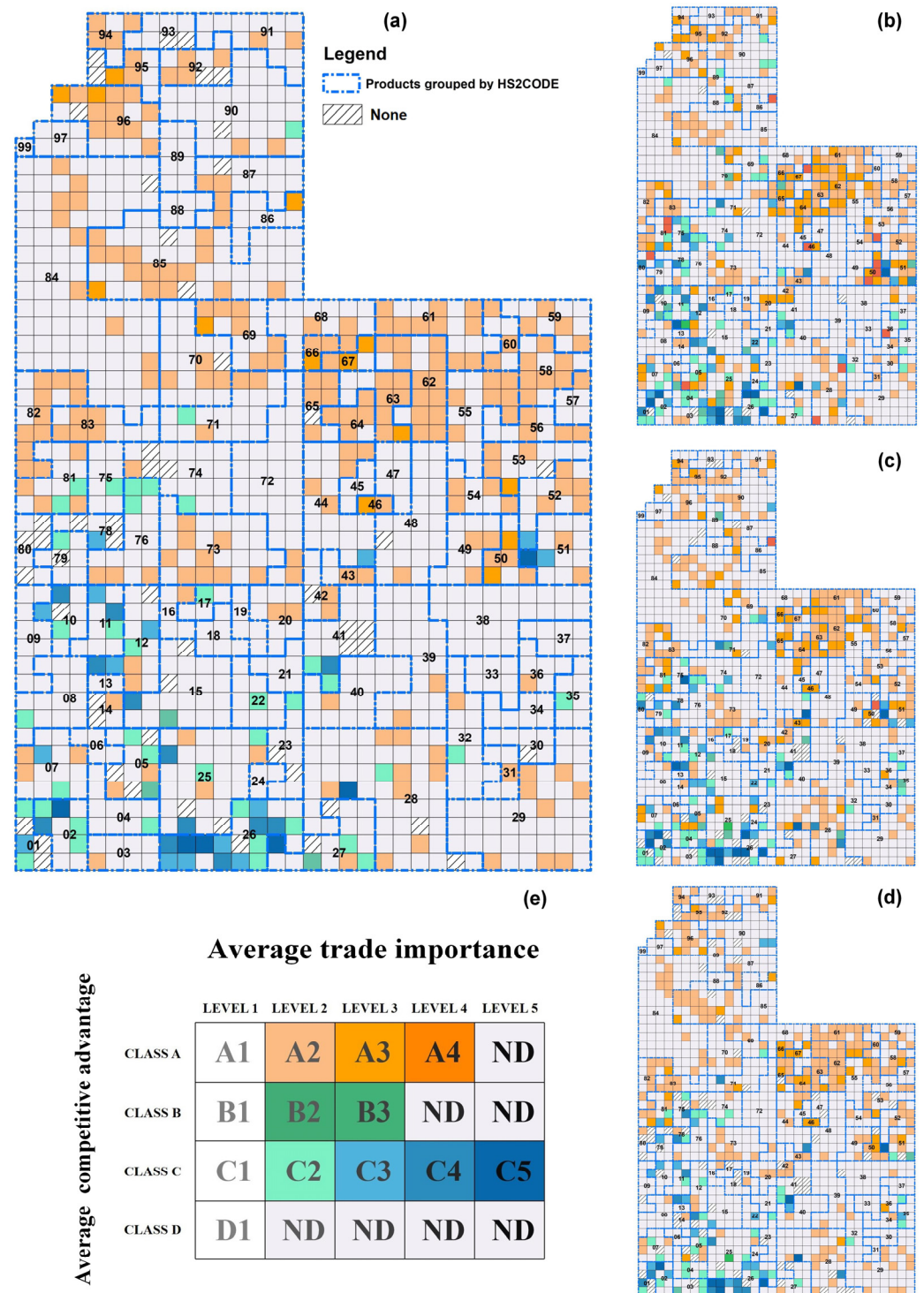


**Figure 7.** Spatial patterns of products’ L (P, i) levels and A (P, i) classes in difference: Colour mapping space of products’ average trade importance and average competitive advantage during the four time periods. Average competitive advantage A (P, i) class information of high-level products (average trade importance L (P, i) level > 1) is expressed in this figure. (a) Spatial pattern of products’ L (P, i) level and A (P, i) class in China–Australia bilateral trade in time period 4 (2011–2019); (b) in time period 1 (1998–2002); (c) in time period 2 (2003–2006); (d) in time period 3 (2007–2010); (e) colour mapping space of L (P, i) level and A (P, i) class. “ND” means no corresponding combination during the four time periods.



## 4. Discussion

### 4.1. Average Importance Index and Competitive Advantage “Changing Pattern”

The HS4CODE of each product was selected as the case classification basis, and the corresponding parameter values of the four periods were used as variables to perform k-means clustering on L (P, i) and A (P, i) (Tables 1 and 2). The optimal number of clusters was determined using the elbow method, as shown in Figure 8, and finally, all three classes were defined. Each class passed the variance test. For L (P, i) (shown in Table 1), nine categories of products (approximately 0.71% of all products) exhibited large initial values, significant variation, and a tendency to increase and decrease significantly over time, eventually decreasing by approximately 25%. A total of 142 categories of products (11.3%) exhibited large initial values, significant variation, and a tendency to decrease constantly over time, eventually decreasing by approximately 44%, while 1105 categories of products (88.0%) showed a small initial value and a small change, with a slow decreasing trend over time and a final decrease of approximately 15%. Overall, the products in each cluster showed a decreasing trend, reflecting the changing pattern of contraction in the importance of trade in products traded between the two countries.

**Table 1.** L (P, i) Cluster centres for k-means analysis.

Time Period	Cluster 1 (n1 = 9)	Cluster2 (n2 = 1105)	Cluster3 (n3 = 142)
1998–2002	29.0142130	1.3675999	8.3746590
2003–2006	33.5533474	1.2112864	7.7501643
2007–2010	27.9883261	1.1526156	6.1057149
2011–2019	21.6110437	1.1589974	4.7332523

**Table 2.** A (P, i) Cluster centres for k-means analysis.

Time Period	Cluster 1 (n1 = 335)	Cluster 2 (n2 = 903)	Cluster 3 (n3 = 18)
1998–2002	72.7118379	16.9254715	−65.9744152
2003–2006	65.6300128	−3.7909736	−93.8163177
2007–2010	75.6674041	10.7797741	−159.7832256
2011–2019	76.1712667	−2.0935835	1.6082544

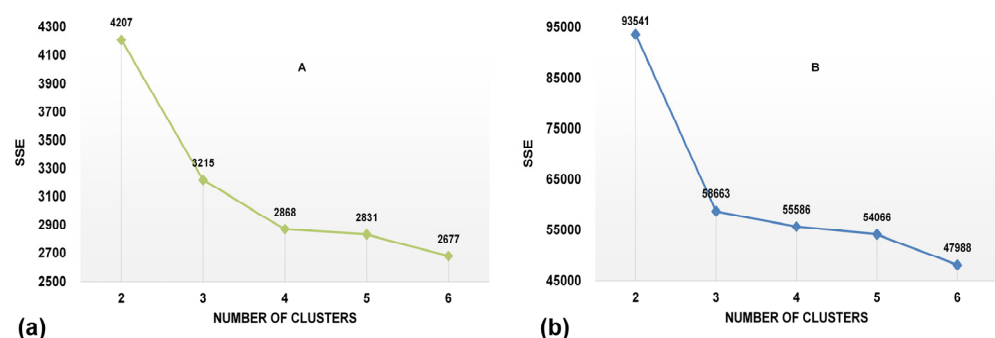


**Figure 8.** K-means clustering results: (a) L (P, i) clustering results' elbow diagram. The sum of squares due to error (SSE) decreases with the increase in the number of clusters and appears when the number of clusters is equal to 3 inflection points. After the inflection point, the total sum of squares within the group changes gently with the increase in the number of clusters. (b) A (P, i) clustering results' elbow diagram.

For A (P, i) (shown in Table 2), 335 products (26.7%) showed an initial period of Australian dominance, with a slight change and an overall trend of expanding Australian dominance. A total of 903 products (71.9%) showed an initial period of Chinese dominance, with a significant change but an overall trend of China's dominance and expanding dominance. A total of 18 products (1.4%) showed that both countries were not dominant in the

initial period, with a wide range of variation, and there was a trend of China gradually gaining advantages over time. Overall, China showed a clear advantage over Australia regarding the number of dominant products, which has been increasing over time.

#### 4.2. Importance Analysis of Head Commodities

The magnitude of the role of essential products in China—Australia trade varies across periods, with products with the highest  $L(P, i)$  levels in the countries' trade playing a significant role in the overall trade at a particular time period. In contrast, the role of these products may not be significant at specific periods. Validating the heavy-tailed distribution, followed by a power-law test for each product in each time period, can be used to explore the significance of those goods with the highest  $L(P, i)$  levels in China—Australia trade, the head products in the heavy-tailed distribution, and the essential products in the overall trade dominance.

Figure 9 shows the results of the power-law test for each time period. The  $R^2$  of the fitted probability density function of each time period is more significant than 0.98 in the double-log plot, which indicates that the products of each time period are consistent with the characteristics of the heavy-tailed distribution. From the first time period (DEGREE 1) to the fourth time period (DEGREE 4), the absolute value of the fitted linear slope tends to decrease first and then increase (from 1.51 to 1.45 and, finally, to 1.98). The dominant role played by the head products in the Chinese ease decreases and then increases with time, and the dominant position becomes important later. This reflects the increasing polarisation of commodities in bilateral trade between Australia and China, as well as the gradual decline in overall stability.

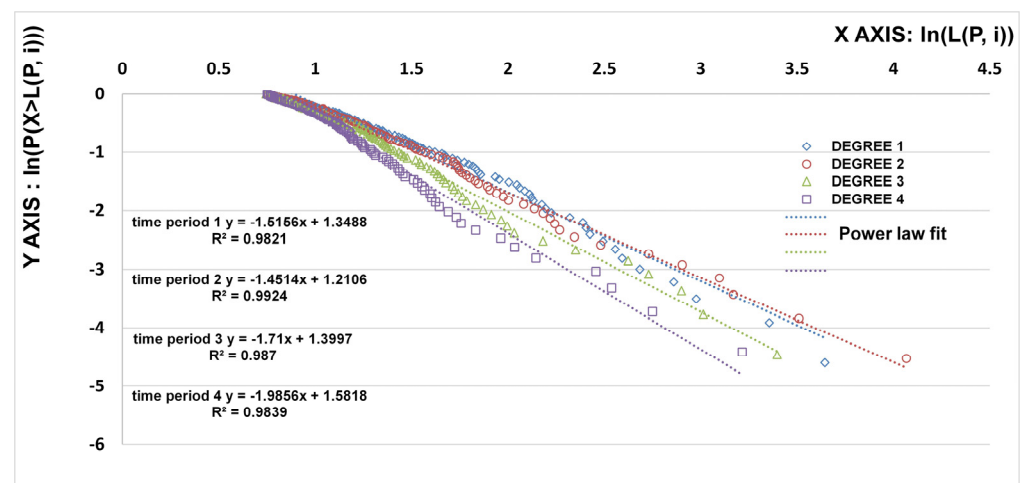


Figure 9. Power-law fit in different time periods.

#### 4.3. Substitution of Dominant Products

With the prevalence of unilateralism, increasing trade barriers, the significant impact of the novel coronavirus epidemic on the world economy since 2020, and the Russia—Ukraine conflict since early 2022, the world trade landscape is deteriorating and moving into unpredictable areas. In recent years, China—Australia bilateral economic and trade cooperation has faced many problems and challenges due to the inevitable impact on China—Australia trade caused by the wave of counter-globalisation, such as the Sino—US trade war and the changes in land-use policy [64,65]. Based on the above background, the search for more exporting countries for the countries' bulk imports can mitigate the impact of the shrinking exports of products due to political and war factors. In Section 3.3, based on the DTFM method, we analysed and showed that the commodities are more critical in China—Australia trade and more advantageous to specific parties. The results show that Australia has the advantage of having the products with the highest importance levels in each segment, and among them, iron ore (HS4CODE = 2601) is even more important. As

a major importer of iron ore, China has been the world's largest iron ore importer since 2003, and most of China's iron ore imports came from Australia by 2020. China needs to find a replacement country for Australian iron ore. We calculated the CA indices of iron ore for the world's major iron-ore-exporting countries at each time and arranged them by percentage.

As shown in Figure 10, iron ore from Australia still holds a considerable advantage at all times, but Brazil also holds a specific share, and its market share is rebounding, while the dominant share of Canadian iron ore has also increased over time. Thus, it would be feasible to import more iron ore from Brazil and Canada, as with China's import of Brazilian iron ore in the first half of 2021. The amount also has a sizeable year-on-year growth.

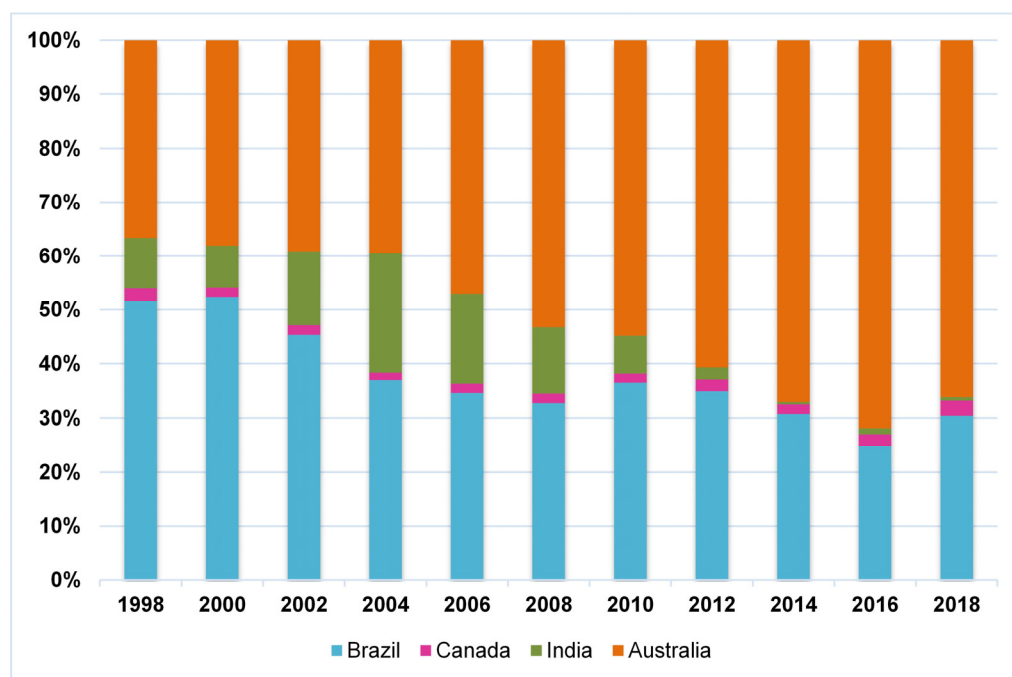


Figure 10. CA indices of different countries from 1998 to 2018.

#### 4.4. Comparison and Outlook

Among the studies conducted by various researchers on China—Australia bilateral trade and changes in China—Australia trade patterns, most of them focus on a particular category of crucial products in China—Australia bilateral trade, such as iron ore [66], energy [67], or agricultural products [40], with less analysis of the overall characteristics of bilateral trade, making it difficult to reveal the patterns of China—Australia bilateral trade from a global perspective (as this study does). In terms of the changing trade patterns between China and Australia, compared to the outlook on the bright future of trade relations between the two countries at the beginning of this century, many scholars have pointed out the tension and degradation of bilateral trade between China and Australia in recent years, with the Sino—US trade war and the tension between China and Australia. Zhou [39] concluded that the China—Australia trade is tense by revealing the underlying factors. After peaking between 2013 and 2015, Australia—China relations declined sharply in 2017 [68]. They have continued to deteriorate since then, reaching a shallow trough from which it seems difficult to escape. Li et al. [66] analysed the iron ore trade conflict between Chinese and Australian firms through a hierarchical dependence expected utility theory model and an asymmetric hawk—dove game, concluding that Australian firms with higher revenues in bilateral trade have a higher probability of resorting to extreme confrontation. The study concluded that pessimism has a more significant impact on the strategic choices of Chinese and Australian firms. These conclusions are consistent with the findings of this study on the “degradation of bilateral trade between Australia and China”. In terms of

research methodology, the “product space” proposed by Hidalgo [69] and the widely used models for analysing product trade patterns—such as the gravity model and the clustering model—often face the problem of constructing networks or clustering models that are too complex when analysing hundreds of products, the difficulty of visualising specific products, and the difficulty of clarifying the differences in trade characteristics between different countries and different stages. It is difficult to clearly express the differences in trade characteristics between countries and stages. DTFM, on the other hand, can analyse and represent the overall pattern of bilateral trade and the evolution of multiple products in a clearer, more operational, and highly scalable way.

In contrast to the original DTFM approach [30], the -co-clustering algorithm was used to delineate the different stages of bilateral trade in order to better analyse changes in trade patterns. In contrast, although the spatial visualisation process of DTFM is not restricted by product type and volume, the constructed trade space can only analyse trade relations between two countries at once. It needs to be able to better analyse the dynamic interactions of trade flows between multiple countries or groups. At the same time, DTFM can only show changes in trade patterns between countries, but it is challenging to directly reveal the reasons for these changes. Based on the existing DTFM, it would be interesting to develop a path-tracing method to characterise the various features of trade relations, identify the types of products that change dramatically and, thus, explore the drivers of sudden changes in bilateral trade.

## 5. Conclusions

In this study, the DTFM method was used to construct a trade space by selecting the competitive advantage index as the analysis index. The co-clustering algorithm was used to classify periods based on trade characteristics. Standard deviation ellipses were constructed to analyse product importance and dominance, and the head/tail breaks method was used to classify products by importance. Finally, Hilbert curve inversions were used to create a digital trade characteristics map representing the “spatial” pattern of trade characteristics. This study analysed the 22-year pattern of bilateral trade between China and Australia from 1998 to 2019. We can conclude that (1) the intensity of trade between China and Australia has gradually decreased over time, as reflected by a 68% decrease in the number of critical products in the fourth period compared to the first period, indicating that the interdependence in trade between China and Australia is weakening; (2) China has always had a competitive advantage in the China—Australia trade relationship, with the share of its dominant products increasing from 71% in the first period to 77% in the fourth period; and (3) in terms of spatial product distribution, the products in which Australia has a competitive advantage are mainly animal products and ores. In contrast, the products in which China has a competitive advantage are mainly labour-intensive light industrial products, and the superior products of both countries show a spatial clustering pattern. At the same time, we believe that (1) Australia has always maintained its competitive advantage in the most critical products in China—Australia trade relations; (2) the phenomenon of product polarisation in China—Australia bilateral trade has become increasingly serious, and the overall trade stability has been declining; and (3) the influence of head products on the overall trade pattern has gradually increased. This paper provides a new method for the study of Sino—Australian trade support. This analytical approach can be extended to analyse the characteristics of bilateral trade between other countries.

This study contributes to the further development of DTFM and trade visualisation methods to enrich the field of China—Australia bilateral trade research by providing a global visualisation of bilateral trade and analysing the declining characteristics and changing advantages of trade between the two countries over more than two decades, based on the improved DTFM method. In the future, we expect to better incorporate the theory of dynamic competitive advantage into the broader practice of DTFM in order to demonstrate changes in the bilateral trade patterns of countries. At the same time, a

path-tracing methodology is expected to be developed to explore the drivers of abrupt changes in bilateral trade from political and economic perspectives.

**Supplementary Materials:** The following supporting information can be downloaded at: <https://www.mdpi.com/article/10.3390/su15097297/s1>, S1: HS 4-digit code grid system. S2: Co-clustering Algorithm [49,70–74]. S3: HS 4-digit code grid system [32]. S4: high-level L (P, i) products details.

**Author Contributions:** Conceptualization, S.Y. and C.S.; Methodology, X.H., S.Y. and S.R.; Software, X.H.; Formal analysis, X.H., S.Y. and S.R.; Resources, C.S.; Data curation, X.H.; Writing—original draft, X.H. and S.Y.; Writing—review & editing, X.H., S.Y. and C.S.; Supervision, X.H., S.Y. and C.S.; Project administration, C.S.; Funding acquisition, C.S. All authors have read and agreed to the published version of the manuscript.

**Funding:** This research was funded by the second Tibetan Plateau Scientific Expedition and Research Program (STEP) (Grant No. 2019QZKK0608), the Strategic Priority Research Program of the Chinese Academy of Sciences (Grant No. XDA23100303), the National Natural Science Foundation of China (Grant No. 42171250), and a Project Supported by the State Key Laboratory of Earth Surface Processes and Resource Ecology (2022-ZD-04).

**Data Availability Statement:** Data available in a publicly accessible repository that does not issue DOIs Publicly available datasets were analyzed in this study. This data can be found here: [<http://comtrade.un.org>].

**Acknowledgments:** We would like to thank the high-performance computing support from the Center for Geodata and Analysis, Faculty of Geographical Science, Beijing Normal University (<https://gda.bnu.edu.cn/> (accessed on 2 August 2022)).

**Conflicts of Interest:** The authors declare no conflict of interest.

## References

- Galama, T.; Hosek, J. *US Competitiveness in Science and Technology*; RAND Corporation: Santa Monica, CA, USA, 2008; Volume 188.
- Wu, Y. The Construction and International Comparison of National Digital Competitiveness Index. *Stat. Res.* **2019**, *36*, 14–25, (In Chinese with English abstract).
- Han, Y.; Luo, X.; Zou, J. Trade Cooperation Competitiveness and Complementarities of China and West Asia under the Background to Silk Road Economic Belt and Maritime Silk Road Strategy. *World Econ. Stud.* **2015**, *3*, 89–98+129, (In Chinese with English Abstract).
- Casanova, C.; Xia, L.; Ferreira, R. Measuring Latin America’s export dependency on China. *J. Chin. Econ. Foreign Trade Stud.* **2016**, *9*, 213–233. [[CrossRef](#)]
- Zhang, Y.; Zhang, X.; Gong, Z. Trade Interdependency Between China and Countries Along the One Belt and One Road. *Econ. Geogr.* **2017**, *37*, 21–31, (In Chinese with English Abstract).
- Tinbergen, J. An analysis of world trade flows. *Shap. World Econ.* **1962**, *3*, 1–117.
- Chen, S.; Huang, Q.; Muttarak, R.; Fang, J.; Liu, T.; He, C.; Liu, Z.; Zhu, L. Updating global urbanization projections under the Shared Socioeconomic Pathways. *Sci. Data* **2022**, *9*, 137. [[CrossRef](#)]
- He, C.; Yu, C. Multi-dimensional proximity, trade barriers and the dynamic evolution of industrial linkages between China and the world marke. *Acta Geogr. Sin.* **2022**, *77*, 275–294, (In Chinese with English Abstract).
- Chapagain, A.K.; Hoekstra, A.Y. The blue, green and grey water footprint of rice from production and consumption perspectives. *Ecol. Econ.* **2011**, *70*, 749–758, (In Chinese with English Abstract). [[CrossRef](#)]
- Fang, D.; Cai, Q.; Wu, F.; Chen, B.; Zhang, L. Modified linkage analysis for water-land nexus driven by interregional trade. *J. Clean. Prod.* **2022**, *353*, 131547. [[CrossRef](#)]
- Yu, X.; Liu, C.; Zhang, G. Market integration and virtual flow of resources under the background of international food trade: Evidence from China-Pakistan rice market. *J. Nat. Resour.* **2021**, *36*, 1505–1520, (In Chinese with English Abstract). [[CrossRef](#)]
- Hoekstra, A.; Mekonnen, M. The water footprint of humanity. *Proc. Natl. Acad. Sci. USA* **2012**, *109*, 3232. [[CrossRef](#)] [[PubMed](#)]
- Sun, S.; Wang, J.; Qi, W. Urban-and-rural virtual water trade of Qinghai-Tibet Plateau: Patterns and influencing factors. *Acta Geogr. Sin.* **2020**, *75*, 1346–1358, (In Chinese with English Abstract).
- Hertwich, E.G.; Peters, G.P. Carbon Footprint of Nations: A Global, Trade-Linked Analysis. *Environ. Sci. Technol.* **2009**, *43*, 6414–6420. [[CrossRef](#)] [[PubMed](#)]
- Peters, G.P.; Minx, J.C.; Weber, C.L.; Edenhofer, O. Growth in emission transfers via international trade from 1990 to 2008. *Proc. Natl. Acad. Sci. USA* **2011**, *108*, 8903–8908. [[CrossRef](#)] [[PubMed](#)]
- Barabas, A.; Albert, R. Emergence of scaling in random networks. *Science* **1999**, *286*, 509–512. [[CrossRef](#)] [[PubMed](#)]
- Hao, X.; An, H.; Chen, Y.; Gao, X. Research on Evolution of International Iron Ore Trade Based on Complex Network Theory. *Econ. Geogr.* **2013**, *33*, 92–97, (In Chinese with English Abstract).

18. Han, M.; Li, S. Network Characteristics and Community Structure of Marine Energy Products Trade Among the Countries Along the Belt and Road. *Econ. Geogr.* **2020**, *40*, 108–117, (In Chinese with English Abstract).
19. Dong, C.; Yin, Q.; Lane, K.J.; Yan, Z.; Shi, T.; Liu, Y.; Bell, M.L. Competition and transmission evolution of global food trade: A case study of wheat. *Phys. A Stat. Mech. Its Appl.* **2018**, *509*, 998–1008. [[CrossRef](#)]
20. Gao, P.; Xie, Y.; Song, C.; Cheng, C.; Ye, S. Exploring detailed urban-rural development under intersecting population growth and food production scenarios: Trajectories for China’s most populous agricultural province to 2030. *J. Geogr. Sci.* **2023**, *33*, 222–244. [[CrossRef](#)]
21. Hao, X.; An, H.; Sun, X.; Zhong, W. The import competition relationship and intensity in the international iron ore trade: From network perspective. *Resour. Policy* **2018**, *57*, 45–54. [[CrossRef](#)]
22. Bai, X.; Hu, X.; Wang, C.; Lim, M.K.; Vilela, A.L.; Ghadimi, P.; Yao, C.; Stanley, H.E.; Xu, H. Most influential countries in the international medical device trade: Network-based analysis. *Phys. A Stat. Mech. Its Appl.* **2022**, *604*, 127889. [[CrossRef](#)]
23. Xu, H.; Sun, T.; Cheng, L. Trade pattern and influencing factors of high-end manufacturing industry in the Belt and Road Initiative: Analysis of Index Random Graph based on complex network. *Financ. Econ.* **2015**, *2015*, 74–88, (In Chinese with English Abstract).
24. Ermann, L.; Shepelyansky, D. Ecological analysis of world trade. *Phys. Lett. A* **2013**, *377*, 250–256. [[CrossRef](#)]
25. Coquidé, C.; Lages, J.; Ermann, L.; Shepelyansky, D.L. COVID-19’s Impact on International Trade. *Entropy* **2022**, *24*, 327. [[CrossRef](#)] [[PubMed](#)]
26. He, C.; Dong, Y.; Zhou, Y. Evolution of export product space in China: Path-dependent or path-breaking? *Acta Geogr. Sin.* **2016**, *71*, 970–983, (In Chinese with English Abstract).
27. Hidalgo, C.; Hausmann, R. The building blocks of economic complexity. *Proc. Natl. Acad. Sci. USA* **2009**, *106*, 10570–10575. [[CrossRef](#)]
28. Hausmann, R.; Klinger, B. The Structure of the Product Space and the Evolution of Comparative Advantage. Working Paper. April 2007. Available online: <http://nrs.harvard.edu/urn-3:HUL.InstRepos:42482358> (accessed on 1 January 2020).
29. Wang, Z.; Guo, T.; Wang, Y. Evolution of Global Aquatic Products Trade Pattern and Influencing Factors from the Perspective of Complex Network. *Areal Res. Dev.* **2022**, *41*, 1–6+13, (In Chinese with English Abstract).
30. Geng, J.; Shen, S.; Cheng, C.; Dai, K. A hybrid spatiotemporal convolution-based cellular automata model (ST-CA) for land-use/cover change simulation. *Int. J. Appl. Earth Obs. Geoinf.* **2022**, *110*, 102789. [[CrossRef](#)]
31. Ye, S.; Ren, S.; Song, C.; Cheng, C.; Shen, S.; Yang, J.; Zhu, D. Spatial patterns of county-level arable land productive-capacity and its coordination with land-use intensity in mainland China. *Agric. Ecosyst. Environ.* **2022**, *326*, 107757. [[CrossRef](#)]
32. Ye, S.; Song, C.; Cheng, C.; Shen, S.; Gao, P.; Zhang, T.; Chen, X.; Wang, Y.; Wan, C. Digital Trade Feature Map: A New Method for Visualization and Analysis of Spatial Patterns in Bilateral Trade. *Int. J. Geo-Inf.* **2020**, *9*, 363. [[CrossRef](#)]
33. Ye, S.; Cheng, C.; Song, C.; Shen, S. Visualizing bivariate local spatial autocorrelation between commodity revealed comparative advantage index of China and USA from a new space perspective. *Environ. Plan. A* **2021**, *53*, 223–226. [[CrossRef](#)]
34. Cai, H. *Characteristics, Trends and Suggestions of Agricultural Trade between China and Australia*; International Economic Cooperation: Tehran, Iran, 2012; pp. 64–67, (In Chinese with English Abstract).
35. Mu, W.; Tong, D. A general model for creating robust choropleth maps. *Comput. Environ. Urban Syst.* **2022**, *96*, 101850. [[CrossRef](#)]
36. Marks, A. An Analysis of the Structure of Trade Between Australia and China: An Australian Perspective. *Econ. Voice* **2020**, *17*, 1–18. [[CrossRef](#)]
37. Wang, Y.; Song, C.; Cheng, C.; Wang, H.; Wang, X.; Gao, P. Modelling and evaluating the economy-resource-ecological environment system of a third-polar city using system dynamics and ranked weights-based coupling coordination degree model. *Cities* **2023**, *133*, 104151. [[CrossRef](#)]
38. Li, H.; Wei, X. Influence of China-Australia FTA on Chinese Dairy Import. *J. Int. Trade* **2011**, *15*, 77–84, (In Chinese with English Abstract).
39. Zhou, W.; Laurenceson, J. Demystifying Australia-China Trade Tensions. *J. World Trade* **2022**, *56*, 51–86. [[CrossRef](#)]
40. Zhang, Y.; Liu, E. *Competitiveness of Agricultural Products Trade between China and Australia*; Guangdong Agricultural Sciences: Guangzhou, China, 2013.
41. Wang, B.; Xiao, H. Factors of fluctuation on China-Australia livestock products trade. *J. China Agric. Univ.* **2016**, *21*, 8.
42. Gao, P.; Gao, Y.; Ou, Y.; McJeon, H.; Zhang, X.; Ye, S.; Wang, Y.; Song, C. Fulfilling global climate pledges can lead to major increase in forest land on Tibetan Plateau. *iScience* **2023**, *26*, 106364. [[CrossRef](#)]
43. Tcha, M.; Wright, D. Determinants of China’s import demand for Australia’s iron ore. *Resour. Policy* **1999**, *25*, 143–149. [[CrossRef](#)]
44. Wang, P.; Ju, J. Comparative Analysis of the China-South Korea and China-Australian Bilateral Trades Commodity Structure. In Proceedings of the 2015 International Conference on Management Science and Management Innovation (MSMI 2015), Guilin, China, 15–16 August 2015; Atlantis Press: Amsterdam, The Netherlands, 2015; pp. 212–217.
45. Gao, P.; Gao, Y.; Zhang, X.; Ye, S.; Song, C. CLUMondo-BNU for simulating land system changes based on many-to-many demand–supply relationships with adaptive conversion orders. *Sci. Rep.* **2023**, *13*, 5559. [[CrossRef](#)]
46. Xiang, H.; Kuang, Y.; Li, C. Impact of the China–Australia FTA on global coal production and trade. *J. Policy Model.* **2017**, *39*, 65–78. [[CrossRef](#)]
47. Mu, W.; Tong, D. Computation of the distance between a polygon and a point in spatial analysis. *Int. J. Geogr. Inf. Sci.* **2022**, *36*, 1575–1600. [[CrossRef](#)]

48. Vollrath, T. *Revealed Competitive Advantage for Wheat*; Staff Reports; United States Department of Agriculture, Economic Research Service: Washington, DC, USA, 1987.
49. Hu, L.; Song, C.; Ye, S.; Gao, P. Spatiotemporal Statistical Imbalance: A Long-Term Neglected Defect in UN Comtrade Dataset. *Sustainability* **2022**, *14*, 1431. [[CrossRef](#)]
50. Minami, M. *Using ArcMap*; ESRI: Redlands, CA, USA, 2002.
51. Zipf, G.K. Human Behaviour and the Principle of Least Effort. *Econ. J.* **1950**, *60*, 808.
52. Jiang, B.; Liu, X. Scaling of geographic space from the perspective of city and field blocks and using volunteered geographic information. *Int. J. Geogr. Inf. Sci.* **2012**, *26*, 215–229. [[CrossRef](#)]
53. Fisher, W. On grouping for maximum homogeneity. *ASA* **1958**, *53*, 789–798. [[CrossRef](#)]
54. Jenks, G.F. Generalization in Statistical Mapping. *Ann. Assoc. Am. Geogr.* **1963**, *53*, 15–26. [[CrossRef](#)]
55. Wang, J.-F.; Li, X.-H.; Christakos, G.; Liao, Y.-L.; Zhang, T.; Gu, X.; Zheng, X.-Y. Geographical detectors-based health risk assessment and its application in the neural tube defects study of the Heshun region, China. *IJGIS* **2010**, *24*, 107–127. [[CrossRef](#)]
56. Jiang, B.; Ma, D. How complex is a fractal? Head/tail breaks and fractional hierarchy. *Geovis. Spat. Anal.* **2018**, *2*, 16. [[CrossRef](#)]
57. Jiang, B.; Yin, J. Ht-Index for Quantifying the Fractal or Scaling Structure of Geographic Features. *Ann. AAG* **2014**, *104*, 530–540. [[CrossRef](#)]
58. Taleb, N. *The Black Swan: The Impact of the Highly Improbable*; Allen Lane: London, UK, 2007.
59. Jiang, B. Head/tail Breaks: A New Classification Scheme for Data with a Heavy-tailed Distribution. *Prof. Geogr.* **2013**, *65*, 482–494. [[CrossRef](#)]
60. Wang, S.; Xu, X. A new algorithm of hilbert scanning matrix and its MATLAB program. *Image Graph.* **2006**, *1*, 119–122.
61. Macqueen, J. Some Methods for Classification and Analysis of MultiVariate Observations. *Proc. Berkeley Symp. Math. Stat.* **1967**, *1*, 281–297.
62. Yang, J.; Zhao, C. Survey on K- Means clustering algorithm. *Comput. Eng. Appl.* **2019**, *55*, 7–14, (In Chinese with English Abstract).
63. Ye, S.; Song, C.; Gao, P.; Liu, C.; Cheng, C. Visualizing clustering characteristics of multidimensional arable land quality indexes at the county level in mainland. *China Environ. Plan. A. Econ. Space* **2022**, *54*, 222–225. [[CrossRef](#)]
64. Huang, M.; Fang, Z. Current situation and future trend of China-Australia economic and trade relations. *Asia-Pac. Econ. Rev.* **2020**, 70–79+150, (In Chinese with English Abstract). [[CrossRef](#)]
65. Ye, S.; Song, C.; Shen, S.; Gao, P.; Cheng, C.; Cheng, F.; Wan, C.; Zhu, D. Spatial pattern of arable land-use intensity in China. *Land Use Policy* **2020**, *99*, 104845. [[CrossRef](#)]
66. Li, W.; Huang, S.; Qi, Y.; An, H. RDEU hawk-dove game analysis of the China-Australia iron ore trade conflict. *Resour. Policy* **2022**, *77*, 102643. [[CrossRef](#)]
67. Wang, B. Current status, new features and recommendations of China-Australia cooperation in minerals and energy. *Contemp. Int. Relat.* **2020**, *30*, 138–153.
68. Mackerras, C. *Australia-China Relations in Decline: An Alternative Viewpoint*; Social Alternatives: Maroochydore, QLD, Australia, 2021; Volume 40, pp. 37–44.
69. Hidalgo, C.A.; Klinger, B.; Barabási, A.-L.; Hausmann, R. The Product Space Conditions the Development of Nations. *Science* **2007**, *317*, 482–487. [[CrossRef](#)]
70. Wu, X.; Zurita-Milla, R.; Kraak, M.-J. Co-clustering geo-referenced time series: Exploring spatio-temporal patterns in Dutch temperature data. *Int. J. Geogr. Inf. Sci.* **2015**, *29*, 624–642. [[CrossRef](#)]
71. Han, J.; Kamber, M.; Pei, J. *Data Mining: Concepts and Techniques*; Morgan Kaufman Publisher: Waltham, MA, USA, 2012; Volume 10, pp. 971–978.
72. Banerjee, A.; Dhillon, I.; Ghosh, J.; Merugu, S.; Modha, D.S. A generalized maximum entropy approach to Bregman Co-clustering and matrix approximation. *J. Mach. Learn. Res.* **2007**, *8*, 1919–1986.
73. Wu, X.; Zurita-Milla, R.; Kraak, M.J. A novel analysis of spring phenological patterns over Europe based on co-clustering. *J. Geophys. Res. Biogeosci.* **2016**, *121*, 1434–1448. [[CrossRef](#)]
74. Cho, H.; Dhillon, I.S.; Guan, Y.; Sra, S. Minimum sum-squared residue co-clustering of gene expression data. In Proceedings of the 2004 SIAM International Conference on Data Mining, Lake Buena Vista, FL, USA, 22–24 April 2004; SIAM: Lake Buena Vista, FL, USA, 2004; pp. 114–125.

**Disclaimer/Publisher’s Note:** The statements, opinions and data contained in all publications are solely those of the individual author(s) and contributor(s) and not of MDPI and/or the editor(s). MDPI and/or the editor(s) disclaim responsibility for any injury to people or property resulting from any ideas, methods, instructions or products referred to in the content.